Proceedings of the 2015
IEEE Conference on Robotics and Biomimetics
Zhuhai, China, December 6-9, 2015

A Rotor-Separated Dynamic Modeling Method for Flexible Manipulators Based on FS-SEA

Peng Chen, Hongyi Li

***Abstract*—A rotor-separated dynamic modelling method is proposed based on the dynamics of spatial operator algebra in this paper, for n-DoF serial flexible-joint manipulators with harmonic reducers and with FS-SEAs (force sourced series elastic actuators) as flexible mechanisms. The completed dynamic model comprises the flexible joint dynamics and the whole arm dynamics. Inverse dynamics and forward dynamics of the two parts are researched respectively, through which the complete rotor-separated dynamic model is finally derived. The modelling method proposed in this paper is verified by simulations. And the simulation results demonstrate the significant advantages of the proposed method.**

I. INTRODUCTION

Compared with rigid manipulators, flexible manipulators have the characteristics of smooth and accurate force control, strong shock resistance and energy storing capacity, for which they exhibit very strong interactive ability [1]. When manipulators interacting with humans, security is the most important precondition. The security precondition requires low impedance at all frequencies, not only in the controllable stable bandwidth [2]. Flexible manipulators can achieve low impedance across the whole frequency domain. That provides essential safety assurance for the interaction between manipulators and humans.

As an effective implementation of flexible manipulators, series elastic actuators (SEA) make joints' flexibility increase significantly through connecting elastic mechanisms into the joints of the manipulators. Pratt and Williamson [3] proposed the concept of SEA for the first time in 1995, and studied its features and control method. Classified according to the control modes, SEAs mainly comprise force sourced ones (FS-SEA) and velocity sourced ones (VS-SEA). By now, there have been some researches already for both of the two kinds of SEA. Sensinger and Weir [4] researched SEA's ability to mimic different stiffness under unconstrained impedance control; Hurst et al [5] developed a variable-compliance actuation system for the problem of biped running based on SEA; Ragonesi et al [6] developed an upper limb exoskeleton driven by SEA for rehabilitation, and researched its control method and performance; Thorson and Caldwell [7] presented a novel revolute nonlinear SEA optimized for highly dynamic tasks, which can be applied to running or jumping of robots. The above are some representative studies on FS-SEA. If a fast inner velocity loop or inner position loop is added over the joint motor, the motor can be regarded as a velocity source [2, 8]. Then the SEA will belong to VS-SEA. The representative studies on VS-SEA include: Vallery et al [8] researched accurate torque control of SEA using cascaded control mode with a fast inner velocity loop under the premise of passivity; Wyeth [9, 10] deeply studied the control issues for VS-SEA, which include control algorithm designing, velocity saturation effect and trajectory generation under saturation, through a kind of self-designed SEA. The main drawback of VS-SEA is that the joint motor can not be regarded as ideal velocity source unconditionally. That is to say the effect of velocity saturation exists. Although the model of VS-SEA is simpler than the one of FS-SEA, the problem of trajectory generation under velocity saturation effect is very complicated. Otherwise, the control structure of double loops also increases the complexity of the system. Consequently, FS-SEA is adopted as the control mode of SEA in this paper.

From literatures and papers, one can still rarely see successful cases of the studies on SEA flexible manipulators by now. The better known are only DLR Hand Arm System from Germany [11], and NASA's Robonaut 2 [1] and Valkyrie [12] from America. But on the modeling problem of SEA flexible manipulators, the above three all have no in-depth discussion. Spong [13] discussed the modeling problem of flexible joint manipulators for the first time in 1987, which has important inspiration significance for modeling flexible manipulators based on SEA. Afterwards, the German Aerospace Center (DLR) inherited Spong's method [14, 15], but did not give further development to it. The modeling method of Spong et al adopts relatively many simplifications, so its consistency with the actual situation is not at a high level. Therefore, this paper will propose a rotor-separated dynamic modeling method for flexible manipulator systems based on FS-SEA, which is highly consistent with the actual situation.

II. SPATIAL OPERATOR ALGEBRA

Spatial operator algebra is a kind of recursive dynamics proposed for series multi-rigid-body systems, which has the advantages of small complexity and being highly

Peng Chen and Hongyi Li are with State Key Laboratory of Robotics, Shenyang Institute of Automation, Chinese Academy of Sciences, Shenyang, 110016, China (corresponding author to provide phone: 0086-24-23970721; e-mail: chenpeng@sia.cn).

Peng Chen is with University of Chinese Academy of Sciences, Beijing, 100049, China.

programmed [16]. Consequently, it is very suitable for the dynamic modeling of multi-DoF series manipulators and the computer programming for the achievement of the dynamic model. The recursive process of spatial operator algebra is simply referred to as follows [16-19]:

The details between adjacent rigid bodies in the model of spatial operator algebra are as shown in Fig. 1.

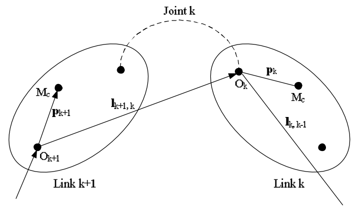

Fig. 1. The details between adjacent rigid bodies in the model of spatial operator algebra

The recursive process of the inverse dynamics is as follows:

$$\begin{aligned} & \boldsymbol{V}_{n+1} = \boldsymbol{V}_{base} \\ & for\ k = n,\dots,1 \\ & \quad \boldsymbol{V}_k = \boldsymbol{\Phi}^T_{k+1,k}\boldsymbol{V}_{k+1} + \boldsymbol{H}_k\dot{\theta}_k \\ & end \end{aligned} \quad , \tag{1}$$

$$\begin{aligned} & \boldsymbol{\alpha}_{n+1} = \boldsymbol{\alpha}_{base} \\ & for\ k = n,\dots,1 \\ & \quad \boldsymbol{\alpha}_k = \boldsymbol{\Phi}^T_{k+1,k}\boldsymbol{\alpha}_{k+1} + \boldsymbol{H}_k\ddot{\theta}_k + \boldsymbol{a}_k \\ & end \end{aligned} \quad , \tag{2}$$

$$\begin{aligned} & \boldsymbol{f}_0 = \boldsymbol{f}_{ext} \\ & for\ k = 1,\dots,n \\ & \quad \boldsymbol{f}_k = \boldsymbol{\Phi}_{k,k-1}\boldsymbol{f}_{k-1} + \boldsymbol{M}_k\boldsymbol{\alpha}_k + \boldsymbol{b}_k; T_k = \boldsymbol{H}_k^T\boldsymbol{f}_k \\ & end \end{aligned} \quad . \tag{3}$$

And the recursive process of the forward dynamics is as follows:

$$\begin{aligned} & \boldsymbol{P}_0^+ = \boldsymbol{0} \\ & for\ k = 1,\dots,n \\ & \quad \boldsymbol{P}_k = \boldsymbol{\Phi}_{k,k-1}\boldsymbol{P}^+_{k-1}\boldsymbol{\Phi}^T_{k,k-1} + \boldsymbol{M}_k; \boldsymbol{D}_k = \boldsymbol{H}_k^T\boldsymbol{P}_k\boldsymbol{H}_k \\ & \quad \boldsymbol{G}_k = \boldsymbol{P}_k\boldsymbol{H}_k\boldsymbol{D}_k^{-1}; \bar{\boldsymbol{\tau}}_k = \boldsymbol{I} - \boldsymbol{G}_k\boldsymbol{H}_k^T; \boldsymbol{P}_k^+ = \bar{\boldsymbol{\tau}}_k\boldsymbol{P}_k \\ & end \end{aligned} \quad , \tag{4}$$

$$\begin{aligned} & \boldsymbol{z}_0^+ = \boldsymbol{f}_{ext} = \boldsymbol{f}_0 \\ & for\ k = 1,\dots,n \\ & \quad \boldsymbol{z}_k = \boldsymbol{\Phi}_{k,k-1}\boldsymbol{z}^+_{k-1} + \boldsymbol{P}_k\boldsymbol{a}_k + \boldsymbol{b}_k; \varepsilon_k = T_k - \boldsymbol{H}_k^T\boldsymbol{z}_k \\ & \quad \nu_k = D_k^{-1}\varepsilon_k; \boldsymbol{z}_k^+ = \boldsymbol{z}_k + \boldsymbol{G}_k\varepsilon_k \\ & end \end{aligned} \quad , \tag{5}$$

$$\begin{aligned} & \boldsymbol{\alpha}_{n+1} = \boldsymbol{\alpha}_{base} \\ & for\ k = n,\dots,1 \\ & \quad \boldsymbol{\alpha}_k^+ = \boldsymbol{\Phi}^T_{k+1,k}\boldsymbol{\alpha}_{k+1}; \ddot{\theta}_k = \nu_k - \boldsymbol{G}_k^T\boldsymbol{\alpha}_k^+ \\ & \quad \boldsymbol{\alpha}_k = \boldsymbol{\alpha}_k^+ + \boldsymbol{H}_k\ddot{\theta}_k + \boldsymbol{a}_k \\ & end \end{aligned} \quad . \tag{6}$$

Thereinto, $\boldsymbol{H}_k$ is the joint matrix for the k-th joint, whose value is directly related to the joint type. For a 1-DoF rotary joint, the form of its joint matrix in the body-fixed coordinate system of the joint is

$${}_k\boldsymbol{H}_k = \begin{bmatrix}0 & 0 & 1 & 0 & 0 & 0\end{bmatrix}^T . \tag{7}$$

$\boldsymbol{\Phi}_{k+1,k}$ is the composite body transformation operator,

$$\boldsymbol{\Phi}_{k+1,k} = \begin{bmatrix}\boldsymbol{I} & \tilde{\boldsymbol{l}}_{k+1,k} \\ \boldsymbol{0} & \boldsymbol{I}\end{bmatrix} . \tag{8}$$

The meanings of $\boldsymbol{a}_k$, $\boldsymbol{b}_k$ and $\boldsymbol{M}_k$ are as follows:

$$\boldsymbol{a}_k = \begin{bmatrix}\tilde{\boldsymbol{\omega}}_{k+1}\boldsymbol{h}_{\omega k}\dot{\theta}_k \\ \tilde{\boldsymbol{\omega}}_{k+1}\tilde{\boldsymbol{\omega}}_{k+1}\boldsymbol{l}_{k+1,k}\end{bmatrix} , \tag{9}$$

$$\boldsymbol{b}_k = \begin{bmatrix}\tilde{\boldsymbol{\omega}}_k\boldsymbol{I}_{k,O}\boldsymbol{\omega}_k \\ m_k\tilde{\boldsymbol{\omega}}_k\tilde{\boldsymbol{\omega}}_k\boldsymbol{p}_k\end{bmatrix} , \tag{10}$$

$$\boldsymbol{M}_k = \begin{bmatrix}\boldsymbol{I}_{k,O} & m_k\tilde{\boldsymbol{p}}_k \\ -m_k\tilde{\boldsymbol{p}}_k & m_k\boldsymbol{I}\end{bmatrix} . \tag{11}$$

The whole process of solving a manipulator's dynamics must be in the same reference coordinate system. In general, we hope to solve the dynamics in the base coordinate system of the manipulator. However, there are some important quantities in spatial operator algebra, such as $\boldsymbol{l}_{k,k-1}$, $\boldsymbol{p}_k$, $\boldsymbol{H}_k$ and $\boldsymbol{I}_{k,O}$, whose forms in the base coordinate system are difficult to be obtained directly. While their forms in the body-fixed coordinate system of the k-th joint ${}_k\boldsymbol{l}_{k,k-1}$, ${}_k\boldsymbol{p}_k$, ${}_k\boldsymbol{H}_k$ and ${}_k\boldsymbol{I}_{k,O}$ are easy to get. They can be transformed from the body-fixed coordinate system of the k-th joint to the base coordinate system with the following transformation relation:

$$\begin{aligned} & \boldsymbol{l}_{k,k-1} = {}^{n+1}\boldsymbol{R}_k\ {}_k\boldsymbol{l}_{k,k-1} \\ & \boldsymbol{p}_k = {}^{n+1}\boldsymbol{R}_k\ {}_k\boldsymbol{p}_k \\ & \boldsymbol{H}_k = \begin{bmatrix}{}^{n+1}\boldsymbol{R}_k & \boldsymbol{0} \\ \boldsymbol{0} & {}^{n+1}\boldsymbol{R}_k\end{bmatrix}{}_k\boldsymbol{H}_k \\ & \boldsymbol{I}_{k,O} = {}^{n+1}\boldsymbol{R}_k\ {}_k\boldsymbol{I}_{k,O}\ {}^{n+1}\boldsymbol{R}_k^T \end{aligned} \quad . \tag{12}$$

In addition, gravity compensation can be easily realized according to the principle of equal effects. The practical approach is adding the vector $[0\ 0\ 0\ 0\ 0\ g]^T$ to the real base acceleration $\boldsymbol{\alpha}_{base}$.

III. ROTOR-SEPARATED DYNAMIC MODELING

A. Rotor Separation

1) The Meaning of Rotor Separation: Restrict the objects to be dynamic modeled to n-DoF series flexible-joint manipulators based on FS-SEA and with harmonic reducers. Because the flexibility of SEA is bigger than that of the harmonic soft round for 1.5 to 2 orders of magnitude in the actual measurement, the flexibility of the harmonic soft round is ignored when modeling. Joint k (k = 1, 2, …, n) of this structure of flexible manipulator can take rotor separation according to Fig. 2. That is, the rotors (including the fast rotor kf and the slow rotor ks) of Joint k are separated out and regarded as independent rigid bodies to be modeled separately. Thus, Joint k can be subdivided into four parts: in the figure Link k + 1 comprises the motor shell, the harmonic support, the harmonic rigid round and the outer ring of the harmonic bearing, which is a part of the (k + 1)-th link of the manipulator; the fast rotor kf includes the motor rotor, the coupler and the wave generator, which rotates fast before the reducer in the motion process of the manipulator; the slow rotor ks includes the harmonic soft round, the inner ring of the harmonic bearing and the input part of SEA, which rotates slowly after the reducer in the motion process of the manipulator; in the figure Link k is the output part of SEA, which is a part of the k-th link of the manipulator. What is particularly noteworthy is that the rotating directions of the fast rotor kf and the slow rotor ks are opposite in the flexible joint with harmonic reducer.

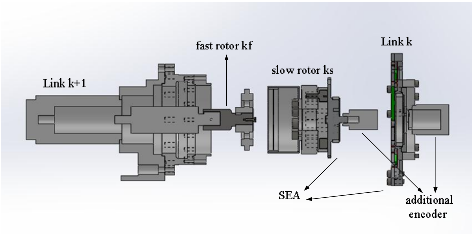

Fig. 2. The rotor-separated model of the k-th flexible joint

After rotor separation to the flexible manipulator to be researched, the properties below can be obtained in combination with the dynamic model of spatial operator algebra.

2) The Force Analysis in the Flexible Joint: As known to all, in the dynamic model of manipulators, every link has its own body-fixed coordinate system. After the rotor separation to the flexible joint, similarly, the body-fixed coordinate systems are built of the separated rotors. The peculiarity of this process is that for the flexible joint k (k = 1, 2, …, n), the origins and the z-axes of the body-fixed coordinate systems of the fast rotor kf and the slow rotor ks all coincide with the counterparts of Link k. From this, the following relations can be obtained:

$$\begin{aligned} \boldsymbol{\Phi}_{k+1,kf} &= \boldsymbol{\Phi}_{k+1,ks} = \boldsymbol{\Phi}_{k+1,k} \\ \boldsymbol{\Phi}_{kf,ks} &= \boldsymbol{\Phi}_{ks,k} = \boldsymbol{\Phi}_{kf,k} = \boldsymbol{I} \end{aligned} , \tag{13}$$

$$\boldsymbol{H}_{kf} = \boldsymbol{H}_{ks} = \boldsymbol{H}_{k} \ . \tag{14}$$

Therefore, the force relationship in the flexible joint k is as follows:

$$\begin{aligned} \boldsymbol{f}_{k+1,kf} &= \boldsymbol{f}_{kf,ks} + \boldsymbol{M}_{kf}\boldsymbol{a}_{kf} + \boldsymbol{b}_{kf} \\ \boldsymbol{f}_{k+1,ks} + \boldsymbol{f}_{kf,ks} &= \boldsymbol{f}_{k} + \boldsymbol{M}_{ks}\boldsymbol{a}_{ks} + \boldsymbol{b}_{ks} \\ \boldsymbol{f}_{k+1} &= \boldsymbol{\Phi}_{k+1,k}\left(\boldsymbol{f}_{k+1,kf} + \boldsymbol{f}_{k+1,ks}\right) + \boldsymbol{M}_{k+1}\boldsymbol{a}_{k+1} + \boldsymbol{b}_{k+1} \end{aligned} , \tag{15}$$

in which $\boldsymbol{f}_r$ denotes the generalized force acting on the rigid body r, $\boldsymbol{f}_{s,\,t}$ denotes the generalized force acting on the rigid body t by the rigid body s.

When the actual force condition inside the joint is not considered and only the accuracy of the joint output force is demanded, the assumption of no force acting between Link k + 1 and the slow rotor ks (k = 1, 2, …, n) can be made. Then the force condition inside the flexible joint k can be regarded as:

$$\begin{aligned} \boldsymbol{f}_{kf,ks} &= \boldsymbol{f}_{k} + \boldsymbol{M}_{ks}\boldsymbol{a}_{ks} + \boldsymbol{b}_{ks} \\ \boldsymbol{f}_{k+1,kf} &= \boldsymbol{f}_{kf,ks} + \boldsymbol{M}_{kf}\boldsymbol{a}_{kf} + \boldsymbol{b}_{kf} \\ \boldsymbol{f}_{k+1} &= \boldsymbol{\Phi}_{k+1,k}\boldsymbol{f}_{k+1,kf} + \boldsymbol{M}_{k+1}\boldsymbol{a}_{k+1} + \boldsymbol{b}_{k+1} \end{aligned} . \tag{16}$$

Under the above assumption, the parts of the flexible joint k after rotor separation turn into a series multi-rigid-body subsystem; and a n-DoF SEA series flexible-joint manipulator will turn into a series multi-rigid-body system containing 3n – 1 rigid bodies (no rotor separation to the joint at the base).

3) The additivity of the acceleration coupled term $\boldsymbol{a}$*:* Extend the definition of the acceleration coupled term $\boldsymbol{a}$, and define the acceleration coupled term from the rigid body s to the rigid body t as

$$\boldsymbol{a}_{s,t} = \begin{bmatrix} \tilde{\boldsymbol{\omega}}_s \boldsymbol{h}_{\omega t}\dot{\theta}_{s,t} \\ \tilde{\boldsymbol{\omega}}_s \tilde{\boldsymbol{\omega}}_s \boldsymbol{l}_{s,t} \end{bmatrix} , \tag{17}$$

in which $\dot{\theta}_{s,t}$ denotes the scalar angular velocity of the rigid body t relative to the rigid body s, around the axis fixed on s. According to the above extended definition, the following relationship can be derived:

$$\begin{aligned} \boldsymbol{a}_{k+1,ks} &= \boldsymbol{a}_{k+1,kf} + \boldsymbol{a}_{kf,ks} \\ \boldsymbol{a}_{kf,k} &= \boldsymbol{a}_{kf,ks} + \boldsymbol{a}_{ks,k} \\ \boldsymbol{a}_{k+1,k} &= \boldsymbol{a}_{k+1,kf} + \boldsymbol{a}_{kf,ks} + \boldsymbol{a}_{ks,k} \end{aligned} . \tag{18}$$

That is, the acceleration coupled term $\boldsymbol{a}$ accords with additivity inside the flexible joint.

B. Flexible Joint Dynamics

1) The Inverse Dynamics of Flexible Joints: It can be obtained from the first two equations of (15) that

$$\begin{aligned} \tau_k &= \boldsymbol{H}_k^T \boldsymbol{f}_{kf,ks} + \boldsymbol{H}_k^T\left(\boldsymbol{M}_{kf}\boldsymbol{a}_{kf} + \boldsymbol{b}_{kf}\right) \\ T_{2,k} &= T_k + \boldsymbol{H}_k^T\left(\boldsymbol{M}_{ks}\boldsymbol{a}_{ks} + \boldsymbol{b}_{ks}\right) \end{aligned} , \tag{19}$$

in which τ_k denotes the driving torque of the motor in the flexible joint k; $T_{2,\,k}$ denotes the total torque applied to the input end of the slow rotor ks (the harmonic soft round); T_k denotes the output torque of the flexible joint k, which is also the output torque of SEA. They satisfy the following relationship respectively:

$$\begin{aligned} \tau_k &= \boldsymbol{H}_k^T \boldsymbol{f}_{k+1,kf} \\ T_{2,k} &= \boldsymbol{H}_k^T\left(\boldsymbol{f}_{k+1,ks} + \boldsymbol{f}_{kf,ks}\right) \\ T_k &= \boldsymbol{H}_k^T \boldsymbol{f}_k = T_{K,k}(\psi_k) + T_{B,k}(\dot{\psi}_k) \end{aligned} . \tag{20}$$

The second equal mark in the third equation denotes that the output torque of SEA comprises two parts of elastic recovery torque and damping torque. The elastic recovery torque is the function of SEA's deformation, and the damping torque is the function of SEA's deformation rate. ψ_k denotes the deformation of SEA, $\psi_k = \varphi_k - \theta_k$, in which φ_k and θ_k denote the angular positions of SEA's input end and output end respectively.

According to the power relationship of harmonic drive, the following equation can be obtained:

$$\boldsymbol{H}_k^T \boldsymbol{f}_{kf,ks}\left(-\mu_k\dot{\varphi}_k\right) = T_{2,k}\dot{\varphi}_k + T_{B2,k}\left(\dot{\varphi}_k\right)\dot{\varphi}_k \ , \tag{21}$$

in which μ_k denotes the harmonic gear ratio in the flexible joint k; $\dot{\varphi}_k$ denotes the output velocity of the harmonic reducer, which is also the rotary velocity of the slow rotor ks; then it can be known from the transmission principle of the harmonic reducer that the input velocity of the harmonic reducer, or the rotary velocity of the fast rotor kf, is $-\mu_k\dot{\varphi}_k$; $T_{B2,k}(\dot{\varphi}_k)$ denotes the damping torque in the process of harmonic drive, which is the function of $\dot{\varphi}_k$.

Combine (19) and (21), the inverse dynamics of the flexible joint based on FS-SEA can be obtained as

$$\begin{aligned}\tau_k &= -\left(T_k + T_{B2,k}(\dot{\varphi}_k) + \boldsymbol{H}_k^T(\boldsymbol{M}_{ks}\boldsymbol{\alpha}_{ks} + \boldsymbol{b}_{ks})\right)/\mu_k \\ &\quad + \boldsymbol{H}_k^T(\boldsymbol{M}_{kf}\boldsymbol{\alpha}_{kf} + \boldsymbol{b}_{kf}), \quad k = 1, 2, \ldots, n\end{aligned} \quad (22)$$

With the inverse dynamics of the flexible joint, the drive torque of the joint motor can be computed out from the related motion status of the flexible joint.

2) The Forward Dynamics of Flexible Joints: Expand $\boldsymbol{\alpha}_{ks}$ and $\boldsymbol{\alpha}_{kf}$ in (22) according to the corresponding formula. After arrangement, the forward dynamics of the flexible joint based on FS-SEA can be obtained as follows:

$$\ddot{\varphi}_k = \frac{-\mu_k\tau_k - T_k - T_{B2,k} - \boldsymbol{H}_k^T\boldsymbol{F}_{ks} + \mu_k\boldsymbol{H}_k^T\boldsymbol{F}_{kf}}{\boldsymbol{I}_{ks,O}(3,3) + \mu_k^2\boldsymbol{I}_{kf,O}(3,3)}, \quad k = 1, 2, \ldots, n \quad (23)$$

in which $\ddot{\varphi}_k$ denotes the output angular acceleration of the harmonic reducer in the flexible joint k, which is also the angular acceleration of SEA's input end; $\boldsymbol{I}_{ks,O}(3,3)$ and $\boldsymbol{I}_{kf,O}(3,3)$ denote the (3, 3) elements of the inertia tensor matrices respectively of the slow rotor ks and the fast rotor kf, with respect to the origins of their own body-fixed frames. $\boldsymbol{F}_{ks}$ and $\boldsymbol{F}_{kf}$ are defined as below:

$$\begin{aligned}\boldsymbol{F}_{ks} &= \boldsymbol{M}_{ks}\boldsymbol{\Phi}_{k+1,k}^T\boldsymbol{\alpha}_{k+1} + \boldsymbol{M}_{ks}\boldsymbol{a}_{k+1,ks} + \boldsymbol{b}_{ks} \\ \boldsymbol{F}_{kf} &= \boldsymbol{M}_{kf}\boldsymbol{\Phi}_{k+1,k}^T\boldsymbol{\alpha}_{k+1} + \boldsymbol{M}_{kf}\boldsymbol{a}_{k+1,kf} + \boldsymbol{b}_{kf}\end{aligned} \quad (24)$$

The forward dynamics of flexible joints shows that the angular acceleration at the input end of the joint's flexible mechanism can be solved out from the drive torque of the joint motor, the position and velocity information inside the flexible joint and the motion status information of the adjacent forestage link.

C. Whole Arm Dynamics

The schema of a series flexible-joint manipulator with n DoFs based on FS-SEA is as shown in Fig. 3.

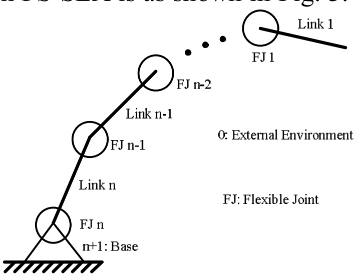

Fig. 3. The schema of a series flexible-joint manipulator with n DoFs based on FS-SEA

1) The Inverse Dynamics of the Whole Arm: The following equation can be derived from (15):

$$\begin{aligned}\boldsymbol{f}_{k+1} &= \boldsymbol{\Phi}_{k+1,k}\boldsymbol{f}_k + \boldsymbol{\Phi}_{k+1,k}(\boldsymbol{M}_{ks}\boldsymbol{\alpha}_{ks} + \boldsymbol{b}_{ks} \\ &\quad + \boldsymbol{M}_{kf}\boldsymbol{\alpha}_{kf} + \boldsymbol{b}_{kf}) + \boldsymbol{M}_{k+1}\boldsymbol{\alpha}_{k+1} + \boldsymbol{b}_{k+1}\end{aligned} \quad (25)$$

Further, the inverse dynamics of the whole arm can be obtained as

$$\begin{aligned}T_k &= \boldsymbol{H}_k^T\boldsymbol{\Phi}_{k,k-1}\boldsymbol{f}_{k-1} + \boldsymbol{H}_k^T\boldsymbol{\Phi}_{k,k-1}(\boldsymbol{M}_{k-1,s}\boldsymbol{\alpha}_{k-1,s} + \boldsymbol{b}_{k-1,s} \\ &\quad + \boldsymbol{M}_{k-1,f}\boldsymbol{\alpha}_{k-1,f} + \boldsymbol{b}_{k-1,f}) + \boldsymbol{H}_k^T(\boldsymbol{M}_k\boldsymbol{\alpha}_k + \boldsymbol{b}_k), \\ k &= 1, 2, \ldots, n\end{aligned} \quad (26)$$

in which all the terms at the right side of the equal mark can be computed with the recursive dynamics of spatial operator algebra. Particularly, when k=1,

$$\boldsymbol{M}_{0s} = \boldsymbol{M}_{0f} = \boldsymbol{0}, \boldsymbol{b}_{0s} = \boldsymbol{b}_{0f} = \boldsymbol{0}, \boldsymbol{f}_0 = \boldsymbol{f}_{ext}. \quad (27)$$

So,

$$T_1 = \boldsymbol{H}_1^T\boldsymbol{\Phi}_{1,0}\boldsymbol{f}_{ext} + \boldsymbol{H}_1^T(\boldsymbol{M}_1\boldsymbol{\alpha}_1 + \boldsymbol{b}_1). \quad (28)$$

With the inverse dynamics of the whole arm, the output torques of the flexible joints, which are also the output torques of SEAs, can be computed out from the motion status of the manipulator links and the motion status inside the flexible joints.

2) The Forward Dynamics of the Whole Arm: In the process of deducing the forward dynamics of the whole arm, the assumption in (16) is applied, because the actual dynamic process inside the joints is not what needs to care about at this time. Then the following relationship can be obtained from the first two equations of (16):

$$\begin{aligned}T_{ks} &= T_k + \boldsymbol{H}_k^T(\boldsymbol{M}_{ks}\boldsymbol{\alpha}_{ks} + \boldsymbol{b}_{ks}) \\ T_{kf} &= T_{ks} + \boldsymbol{H}_k^T(\boldsymbol{M}_{kf}\boldsymbol{\alpha}_{kf} + \boldsymbol{b}_{kf})\end{aligned} \quad (29)$$

Based on the assumption of (16), the forward dynamics recursive process of spatial operator algebra is applied to the series multi-rigid-body system after the conversion, and the recursive algorithm of the whole arm forward dynamics for FS-SEA flexible manipulators is obtained as follows:

$$\begin{aligned}
&\boldsymbol{D}_1 = \boldsymbol{H}_1^T\boldsymbol{M}_1\boldsymbol{H}_1; \boldsymbol{G}_1 = \boldsymbol{M}_1\boldsymbol{H}_1\boldsymbol{D}_1^{-1} \\
&\bar{\boldsymbol{\tau}}_1 = \boldsymbol{I} - \boldsymbol{G}_1\boldsymbol{H}_1^T; \boldsymbol{P}_1^+ = \bar{\boldsymbol{\tau}}_1\boldsymbol{M}_1 \\
&\mathit{for}\ k = 1, \ldots, n-1 \\
&\quad \boldsymbol{P}_{ks} = \boldsymbol{P}_k^+ + \boldsymbol{M}_{ks}; \boldsymbol{D}_{ks} = \boldsymbol{H}_k^T\boldsymbol{P}_{ks}\boldsymbol{H}_k \\
&\quad \boldsymbol{G}_{ks} = \boldsymbol{P}_{ks}\boldsymbol{H}_k\boldsymbol{D}_{ks}^{-1}; \bar{\boldsymbol{\tau}}_{ks} = \boldsymbol{I} - \boldsymbol{G}_{ks}\boldsymbol{H}_k^T \\
&\quad \boldsymbol{P}_{ks}^+ = \bar{\boldsymbol{\tau}}_{ks}\boldsymbol{P}_{ks}; \boldsymbol{P}_{kf} = \boldsymbol{P}_{ks}^+ + \boldsymbol{M}_{kf} \\
&\quad \boldsymbol{D}_{kf} = \boldsymbol{H}_k^T\boldsymbol{P}_{kf}\boldsymbol{H}_k; \boldsymbol{G}_{kf} = \boldsymbol{P}_{kf}\boldsymbol{H}_k\boldsymbol{D}_{kf}^{-1} \\
&\quad \bar{\boldsymbol{\tau}}_{kf} = \boldsymbol{I} - \boldsymbol{G}_{kf}\boldsymbol{H}_k^T; \boldsymbol{P}_{kf}^+ = \bar{\boldsymbol{\tau}}_{kf}\boldsymbol{P}_{kf} \\
&\quad \boldsymbol{P}_{k+1} = \boldsymbol{\Phi}_{k+1,k}\boldsymbol{P}_{kf}^+\boldsymbol{\Phi}_{k+1,k}^T + \boldsymbol{M}_{k+1} \\
&\quad \boldsymbol{D}_{k+1} = \boldsymbol{H}_{k+1}^T\boldsymbol{P}_{k+1}\boldsymbol{H}_{k+1}; \boldsymbol{G}_{k+1} = \boldsymbol{P}_{k+1}\boldsymbol{H}_{k+1}\boldsymbol{D}_{k+1}^{-1} \\
&\quad \bar{\boldsymbol{\tau}}_{k+1} = \boldsymbol{I} - \boldsymbol{G}_{k+1}\boldsymbol{H}_{k+1}^T; \boldsymbol{P}_{k+1}^+ = \bar{\boldsymbol{\tau}}_{k+1}\boldsymbol{P}_{k+1} \\
&\mathit{end}
\end{aligned} \quad , \quad (30)$$

$$\begin{aligned}
&\boldsymbol{z}_1 = \boldsymbol{\Phi}_{1,0}\boldsymbol{f}_{ext} + \boldsymbol{M}_1\boldsymbol{a}_{1s,1} + \boldsymbol{b}_1; \varepsilon_1 = T_1 - \boldsymbol{H}_1^T\boldsymbol{z}_1 \\
&\nu_1 = D_1^{-1}\varepsilon_1; \boldsymbol{z}_1^+ = \boldsymbol{z}_1 + \boldsymbol{G}_1\varepsilon_1 \\
&\mathit{for}\ k = 1, \ldots, n-1 \\
&\quad \boldsymbol{z}_{ks} = \boldsymbol{z}_k^+ + \boldsymbol{P}_{ks}\boldsymbol{a}_{kf,ks} + \boldsymbol{b}_{ks}; \varepsilon_{ks} = T_{ks} - \boldsymbol{H}_k^T\boldsymbol{z}_{ks} \\
&\quad \boldsymbol{z}_{ks}^+ = \boldsymbol{z}_{ks} + \boldsymbol{G}_{ks}\varepsilon_{ks}; \boldsymbol{z}_{kf} = \boldsymbol{z}_{ks}^+ + \boldsymbol{P}_{kf}\boldsymbol{a}_{k+1,kf} + \boldsymbol{b}_{kf} \\
&\quad \varepsilon_{kf} = T_{kf} - \boldsymbol{H}_k^T\boldsymbol{z}_{kf}; \boldsymbol{z}_{kf}^+ = \boldsymbol{z}_{kf} + \boldsymbol{G}_{kf}\varepsilon_{kf} \\
&\quad \boldsymbol{z}_{k+1} = \boldsymbol{\Phi}_{k+1,k}\boldsymbol{z}_{kf}^+ + \boldsymbol{P}_{k+1}\boldsymbol{a}_{(k+1)s,k+1} + \boldsymbol{b}_{k+1}; \varepsilon_{k+1} = T_{k+1} - \boldsymbol{H}_{k+1}^T\boldsymbol{z}_{k+1} \\
&\quad \nu_{k+1} = D_{k+1}^{-1}\varepsilon_{k+1}; \boldsymbol{z}_{k+1}^+ = \boldsymbol{z}_{k+1} + \boldsymbol{G}_{k+1}\varepsilon_{k+1} \\
&\mathit{end}
\end{aligned} \quad ,(31)$$

$$
\begin{aligned}
&\boldsymbol{\alpha}_n^+ = \boldsymbol{\Phi}_{n+1,n}^T \boldsymbol{\alpha}_{base};\ddot{\theta}_n = v_n - \boldsymbol{G}_n^T \boldsymbol{\alpha}_n^+ \\
&\boldsymbol{\alpha}_n = \boldsymbol{\alpha}_n^+ + \boldsymbol{H}_n \ddot{\theta}_n + \boldsymbol{a}_{n+1,n} \\
&for\ k = n-1,\ldots,1 \\
&\quad \boldsymbol{\alpha}_k^+ = \boldsymbol{\Phi}_{k+1,k}^T \boldsymbol{\alpha}_{k+1} + \boldsymbol{H}_k \ddot{\varphi}_k + \boldsymbol{a}_{k+1,ks} \\
&\quad \ddot{\theta}_k = \ddot{\varphi}_k + v_k - \boldsymbol{G}_k^T \boldsymbol{\alpha}_k^+ \\
&\quad \boldsymbol{\alpha}_k = \boldsymbol{\alpha}_k^+ + \boldsymbol{H}_k \left(\ddot{\theta}_k - \ddot{\varphi}_k\right) + \boldsymbol{a}_{ks,k} \\
&end
\end{aligned}
\quad . \qquad (32)
$$

With the forward dynamics of the whole arm, the accelerations of the manipulator's links, which are also the output angular accelerations of the flexible joints, can be computed out from the output torques of the manipulator's joints, the position and velocity information of the manipulator's links and the motion status information inside the flexible joints.

IV. Simulations

For series flexible-joint manipulators based on FS-SEA researched in this paper, their dynamics is divided into two parts of the flexible joint dynamics and the whole arm dynamics in the above. The cascade method will be adopted to calculate the control torques or the motion status of the manipulator. It can be found from the rotor-separated dynamic model proposed in this paper that the flexible joint dynamics and the whole arm dynamics couple together. That is, when calculating with the cascade method, the case will happen that some quantities need to be used as known before they are determined. This contradiction can be effectively resolved with Adams prediction-correction method [20].

The simulation object is an emulational flexible manipulator with 3 joints. Its schema is as shown in Fig. 4. All the 3 joints of the manipulator are flexible joints based on FS-SEA. For the 3 joints of the manipulator, the expected motion curves are appointed simultaneously. Compute the corresponding motor output torques with the inverse dynamics, then substitute the motor output torques into the forward dynamics to compute the actual motion curves of the manipulator, and finally compare the actual motion curves with the expected motion curves. The expected motion curves of the manipulator's joints are given in Fig. 5.

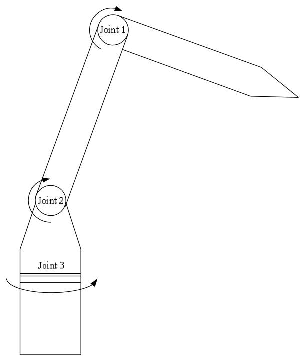

Fig. 4. The schema of the simulation object

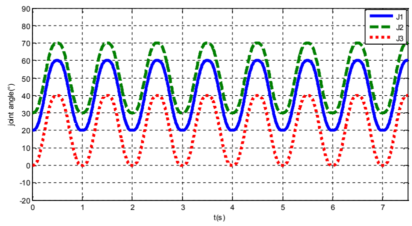

Fig. 5. The expected trajectories of manipulator joints in the simulation

For comparison, take simulations with the method proposed in this paper and with DLR's method [14, 15] respectively. The comparison situations between the actual motion curves and the expected motion curves of the emulational manipulator's 3 joints are as shown in Fig. 6 – 8 respectively, and the tracking error situations of each joint are as shown in Fig. 9 – 11 respectively.

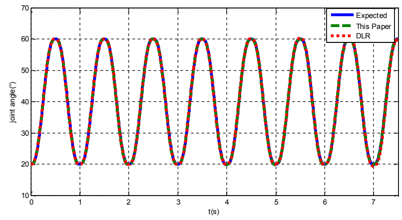

Fig. 6. The comparison between the actual trajectories and the expected trajectory of Joint 1

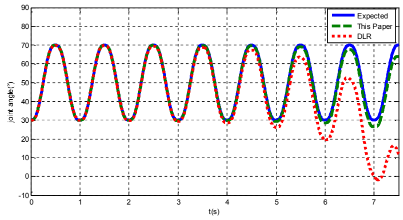

Fig. 7. The comparison between the actual trajectories and the expected trajectory of Joint 2

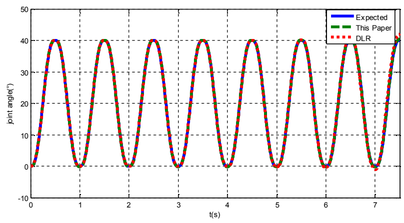

Fig. 8. The comparison between the actual trajectories and the expected trajectory of Joint 3

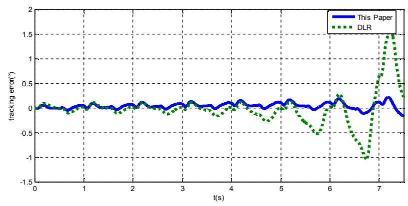

Fig. 9. The tracking errors of Joint 1

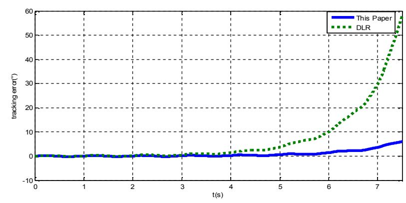

Fig. 10. The tracking errors of Joint 2

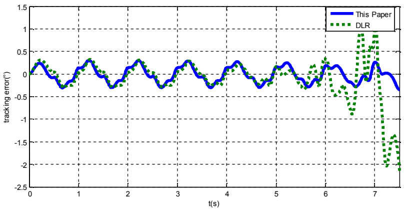

Fig. 11. The tracking errors of Joint 3

It can be seen from the simulation results that the trajectory tracking effect with the dynamic model proposed in this paper is much better than the effect with the dynamic model used by DLR, for the flexible-joint manipulator based on FS-SEA under the condition of no feedback. This indicates that the dynamic model for flexible-joint manipulators proposed in this paper accords with the actual situations better.

V. CONCLUSIONS

This paper proposes a rotor-separated dynamic modelling method based on the dynamics of spatial operator algebra, for n-DoF serial flexible-joint manipulators with harmonic reducers and with FS-SEAs as flexible mechanisms. The completed dynamic model comprises the flexible joint dynamics and the whole arm dynamics. The modeling method proposed in this paper is verified by simulations, and compared with the dynamic model employed by DLR. The simulation results demonstrate the significant advantages of the proposed modeling method.

The dynamic model proposed in this paper possesses 3 remarkable superiorities as below: 1. the physical processes at the joints of flexible manipulators are very clear and definite; 2. the calculation results are more accurate, because of the more detailed dynamic modeling; 3. the inverse dynamic model and the forward dynamic model are proposed simultaneously, which both have a relatively low computation complexity.

REFERENCES

[1] M. A. Diftler, J. S. Mehling, M. E. Abdallah, et al, "Robonaut 2 - The First Humanoid Robot in Space," in *Robotics and Automation (ICRA), 2011 IEEE International Conference on*, Shanghai, PEOPLES R CHINA, 2011, pp. 2178-2183.

[2] J. W. Sensinger, R. F. Weir, "Improvements to Series Elastic Actuators," in *Mechatronic and Embedded Systems and Applications, Proceedings of the 2nd IEEE/ASME International Conference on*, Beijing, PEOPLES R CHINA, 2006, pp. 160- 166.

[3] G. A. Pratt , M. M. Williamson, "Series Elastic Actuators," in *1995 IEEE/RSJ International Conference on Intelligent Robots and Systems - Human Robot Interaction and Cooperative Robots*, Pittsburgh, PA, vol. 1, 1995, pp. 399-406.

[4] J. W. Sensinger, R. F. Weir, "Unconstrained impedance control using a compact series elastic actuator," in *Mechatronic and Embedded Systems and Applications, Proceedings of the 2nd IEEE/ASME International Conference on*, Beijing, PEOPLES R CHINA, 2006, pp. 167-172.

[5] J. W. Hurst, J. E. Chestnutt, A. A. Rizzi, "The Actuator With Mechanically Adjustable Series Compliance," in *IEEE Transactions on Robotics*, vol. 26, no. 4, 2010, pp. 597-606.

[6] D. Ragonesi, S. Agrawal, W. Sample, T. Rahman, "Series Elastic Actuator Control of a Powered Exoskeleton," in *33rd Annual International Conference of the IEEE Engineering in Medicine and Biology Society (EMBS)*, Boston, MA, 2011, pp. 3515-3518.

[7] Ivar Thorson, D. Caldwell, "A Nonlinear Series Elastic Actuator for Highly Dynamic Motions," in *Intelligent Robots and Systems (IROS), 2011 IEEE/RSJ International Conference on*, San Francisco, CA, 2011, pp. 390-394.

[8] H. Vallery, R. Ekkelenkamp, H. van der Kooij, M. Buss, "Passive and Accurate Torque Control of Series Elastic Actuators," in *IEEE/RSJ International Conference on Intelligent Robots and Systems*, San Diego, CA, 2007, pp. 3534-3538.

[9] Gordon Wyeth, "Control Issues for Velocity Sourced Series Elastic Actuators," in *Proceedings of the 2006 Australasian Conference on Robotics & Automation*, Auckland, New Zealand, 2006.

[10] Gordon Wyeth, "Demonstrating the Safety and Performance of a Velocity Sourced Series Elastic Actuator," in *IEEE International Conference on Robotics and Automation*, Pasadena, CA, 2008, pp. 3642-3647.

[11] F. Petit, A. Albu-Schaffer, "State Feedback Damping Control for a Multi DOF Variable Stiffness Robot Arm," in *2011 IEEE International Conference on Robotics and Automation (ICRA 2011)*, Shanghai, China, 2011, pp. 5561–5567.

[12] N. Paine, J. S. Mehling, J. Holley, et al, "Actuator Control for the NASA-JSC Valkyrie Humanoid Robot: A Decoupled Dynamics Approach for Torque Control of Series Elastic Robots," in *JOURNAL OF FIELD ROBOTICS*, vol. 32, no. 3, 2015, pp. 378-396.

[13] M. W. Spong, "Modeling and Control of Elastic Joint Robots," in *Transactions of the ASME. Journal of Dynamic Systems, Measurement and Control*, vol. 109, no. 4, 1987, pp. 310-319.

[14] A. Albu-Schaeffer, C. Ott, G. Hirzinger, "A Unified Passivity-based Control Framework for Position, Torque and Impedance Control of Flexible Joint Robots," in *INTERNATIONAL JOURNAL OF ROBOTICS RESEARCH*, vol. 26, no. 1, 2007, pp. 23-39.

[15] C. Ott, A. Albu-Schaffer, A. Kugi, G. Hirzinger, "On the Passivity-Based Impedance Control of Flexible Joint Robots," in *IEEE TRANSACTIONS ON ROBOTICS*, vol. 24, no. 2, 2008, pp. 416-429.

[16] W. L. Li, Z. N. Yu, P. Shi, Y. S. Zhao, "Recursive Finite Segment Method Analysis of Flexible Spacecraft Undergoing Large Overall Motions," in *Chinese Space Science and Technology*, vol. 32, no. 4, 2012, pp. 22-28.

[17] A. JAIN, "Unified Formulation of Dynamics for Serial Rigid Multibody Systems," in *JOURNAL OF GUIDANCE CONTROL AND DYNAMICS*, vol. 14, no. 3, 1991, pp. 531-542.

[18] G. RODRIGUEZ, A. JAIN, K. KREUTZDELGADO, "Spatial Operator Algebra for Multibody System Dynamics," in *JOURNAL OF THE ASTRONAUTICAL SCIENCES*, vol. 40, no. 1, 1992, pp. 27-50.

[19] Z. X. Tian, "Research on Mutibody Dynamics and Target Capturing for Free-Floating Space Robot," Nanjing University of Aeronautics and Astronautics, 2012.

[20] X. G. Wang, "The Annotation About Prediction - Correction Method," in *Journal of Mathematics For Technology*, vol. 10, no. 3, 1994, pp. 85-86.